High Efficient Solar Power System Using MPPT for Industrial Applications

Miss. Jovis George[1] Miss. Monica[2]
[1]M.E Student [2]Assistant Professor
[1,2]Department of Power Electronics and Drives
[1]CSI College of Engineering, Ketty

Abstract— There has been a rapid increase in the usage of renewable energy resources due to disappearance of coal and oil. Thus solar power is one among these resources. This project focuses on designing of Photovoltaic (PV) cell and its parameters. From the literature survey it was clear that incremental conductance algorithm is easy method and works better than other maximum power point tracking algorithm. Hence incremental conductance technique is used to track maximum power from PV cell. The boost converter gives good performance among various types of DC to DC converters for a PV system. It can also provide a better output current characteristic due to the inductor on the output stage. Thus DC-DC with voltage multiplier module is chosen for DC to DC conversion. A fixed-step-size incremental conductance MPPT with direct control method is employed and necessity of another control loop is eliminated. MATLAB and Simulink will be employed for simulation and analysis of the DC-DC converter for PV power system using incremental conductance technique novel high intensify converter, which is suitable for renewable energy system, is proposed in this project. Through a voltage multiplier module composed of switched capacitors and coupled inductors. The configuration of the proposed converter not only reduces the current stress but also constrains the input current ripple, which decreases the conduction losses and lengthens the lifetime of the input source. In addition, due to the lossless passive clamp performance, leakage energy is recycled to the output terminal. Hence, large voltage spikes across the main switches are alleviated, and the efficiency is improved. For the grid connected application dc output is connected to the efficient inverter.

Key words: MATLAB, Conversion of Solar Energy, Maximum Power Point Tracking (MPPT)

I. INTRODUCTION

Among the renewable energy resources, the energy through the solar photovoltaic effect can be considered the most necessary and prerequisite sustainable resource because of the ubiquity, large quantity, and sustainability of solar energy. The output characteristics of PV module depends on the solar irradiance, cell temperature and output voltage of PV module. Solar energy is an important part of life. Since solar energy is completely natural, it is considered a clean energy source. It does not disrupt the environment or create a threat to Eco-systems the way oil and some other energy sources might. It does not cause greenhouse gases, air or water pollution. The small amount of impact it does have on the environment is usually from the chemicals and solvents that are used during the manufacture of the photovoltaic cells that are needed to convert the sun's energy into electricity. This is a small problem compared to the huge impact that one oil spill can have on the environment.

In the future, solar energy may well be the primary form of energy. This could lead to a clean environment, less money spent on utilities, and a healthier world.

A. Applications of Solar System

Solar technologies are broadly qualified as either passive or active depending on the way they catch, change over and distribute sunlight. Active solar proficiencies use chemical industries photovoltaic arrays, pumps, and fans to convert sunlight into executable outputs. Passive solar techniques include selecting materials with favorable thermal attributes, and citing the position of a building to the sun. The standalone PV Systems have been used for solar street lighting, home lighting system, SPV water pumping system. A hybrid system installed with a backup system of diesel generator can be used in remote military installations, health centers and tourist bungalows. In grid connected system the major part of the load during the day is supplied by the PV array and then from the grid when the sunlight is not sufficient.

Since PV module has nonlinear characteristics, it is necessary to model it and simulate for Maximum Power Point Tracking (MPPT) of PV system applications. A PV module generates small power, so the task of a MPPT in a PV energy conversion system is to continuously tune the system so that it draws maximum power from the solar array regardless of weather or load conditions PV energy conversion system is to continuously tune the system so that it draws maximum power from the solar array regardless of weather or load conditions.

Theoretically, conventional step-up converters, such as the boost converter and fly back converter, cannot achieve a high step-up conversion with high efficiency because of the resistances of elements or leakage inductance also, the voltage stresses are large.

The high step-up single-switch converters are unsuitable to operate at heavy load given a large input current ripple, which increases conduction losses. The conventional interleaved boost converter is an excellent candidate for high-power applications and power factor correction. Unfortunately, the step-up gain is limited, and the voltage stresses on semiconductor components are equal to output voltage. Hence, based on the aforementioned considerations, modifying a conventional interleaved boost converter for high step-up and high-power application is a suitable approach.

To integrate switched capacitors into an interleaved boost converter may make voltage gain reduplicate, but no employment of coupled inductors causes the step-up voltage gain to be limited. Oppositely, to integrate only coupled inductors into an interleaved boost converter may make voltage gain higher and adjustable, but no employment of switched capacitors causes the step-up voltage gain to be ordinary. Thus, the synchronous employment of coupled

inductors and switched capacitors is a better concept moreover high step-up gain, high efficiency, and low voltage stress is achieved even for high-power applications.

II. CONVERSION OF SOLAR ENERGY

Solar energy became one of important resource of energy generation. When solar cells are exposed to sunlight, it converts solar energy into electrical energy and sent to loads or charges the battery bank. The DC power can be converted to AC by means inverter and can be used for standalone or grid connected system.

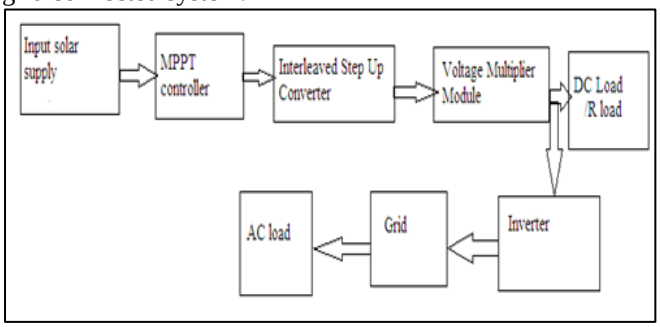

Fig. 1: Block Diagram Efficient for Solar Power System

A. Maximum Power Point Tracking Technique:

A typical solar panel converts only 30 to 40 percent of the incident solar irradiation into electrical energy. Maximum power point tracking technique is used to improve the efficiency of the solar panel. A MPPT is used for extracting the maximum power from the solar PV module and transferring that power to the load. MPPT is an electronic system that operates the PV modules in a manner that allows the modules to produce all the power they are capable of. MPPT is not a mechanical tracking system that "physically moves" the modules to make them point more directly at the sun. MPPT is a fully electronic system that varies the electrical operating point of the modules so that the modules are able to deliver maximum available power.

According to Maximum Power Transfer theorem, the power output of a circuit is maximum when the They are in impedance of the circuit (source impedance) matches with the load impedance. Hence the maximum power point tracking reduces to an impedance matching problem. In the source side we are using a boost convertor connected to a solar panel in order to enhance the output voltage so that it can be used for different applications like motor load. By changing the duty cycle of the boost converter appropriately we can match the source impedance with that of the load impedance. In general MPPT methods can be classified as:

- The first category is Voltage feedback based methods which compare the PV operating voltage with a reference voltage in order to generate the PWM control signal of the DC-DC converter.
- The second category is Current feedback based methods which use the PV module short circuit current as a feedback in order to estimate the optimal current corresponding to the maximum power.
- The third category is Power based methods which are based on iterative algorithms to track continuously the MPP through current and voltage measurement of the PV module. In this category, one of the most successful and used method is perturbation and observation.

B. Incremental Conductance Method:

In this method, the array terminal voltage is always adjusted according to the MPP voltage. It is based on the incremental and instantaneous conductance of the PV module. The disadvantage of perturb and observe method to track the peak power under fast varying atmospheric condition is overcome by IC method. The IC can determine that the MPPT has reached the MPP and stop perturbing the operating point.

The IC can determine that the MPPT has reached the MPP and stop perturbing the operating point. If this condition is not met, the direction in which the MPPT operating point must be perturbed can be calculated using the relationship between dI/dV and –I/V This relationship is derived from the fact that dP/dV is negative when the MPPT is to the right of the MPP and positive when it is to the left of the MPP. This algorithm has advantages over P&O in that it can determine when the MPPT has reached the MPP, where P&O oscillates around the MPP. Also, incremental conductance can track rapidly increasing and decreasing irradiance conditions with higher accuracy than P&O.

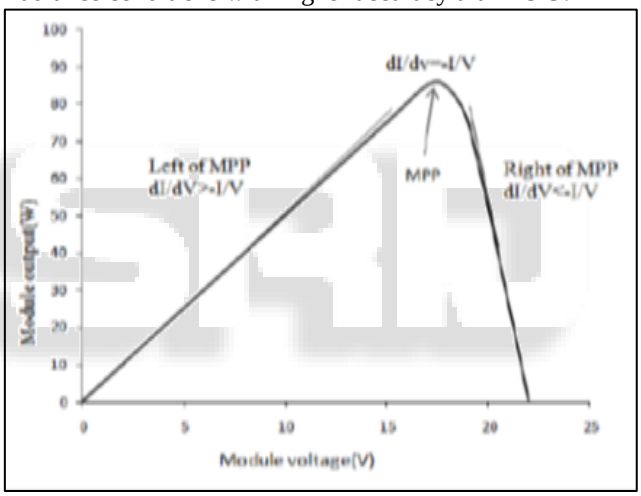

Fig. 2: PV Curve of Solar Panel

The slope of the PV array power curve is zero at the MPP, increasing on the left of the MPP and decreasing on the right-hand side of the MPP. The basic equations of this method are as follows:

$$\frac{dI}{dV} = -\frac{I}{V}, \quad \text{at MPP} \qquad (3.3)$$

$$\frac{dI}{dV} > -\frac{I}{V}, \quad \text{left of MPP} \qquad (3.4)$$

$$\frac{dI}{dV} < -\frac{I}{V}, \quad \text{right of MPP} \qquad (3.5)$$

Where, I = The PV array output current.
V = The PV array output voltage.

The left-hand side of the equations represents the Incremental Conductance of the PV module, and the right-hand side represents the instantaneous conductance. From (3.3)–(3.5), it is obvious that when the ratio of change in the output conductance is equal to the negative output conductance, the solar array will operate at the MPP.

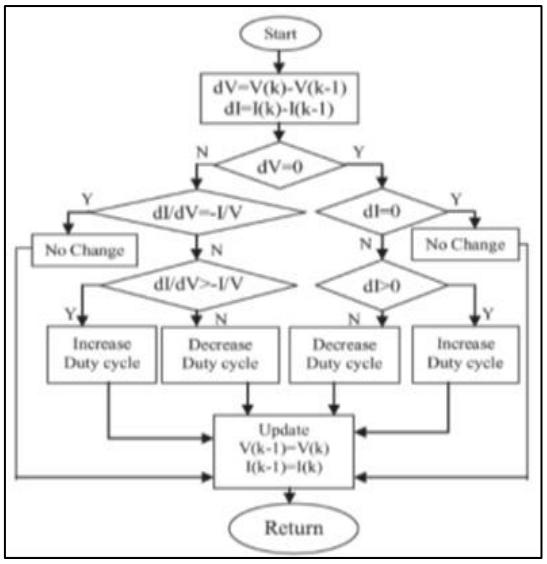

Fig. 3: Flow Chart of Incremental Conductance

In other words, by comparing the conductance at each sampling time, the MPPT will track the maximum power of the PV module. The accuracy of this method is proven in, where it mentions that the incremental conductance method can track the true MPPs independent of PV array characteristics. The main advantage of this algorithm over the P&O method is its fast power tracking process. However, it has the disadvantage of possible output instability due to the use of derivative algorithm. Also the differentiation process under low levels of insolation becomes difficult and results are unsatisfactory.

III. MODELING AND ANALYSIS OF INTERLEAVED CASCADED CONVERTER

A. Circuit Diagrams:

The proposed high step-up interleaved converter with a voltage multiplier module. The voltage multiplier module is composed of two coupled inductors and two switch capacitors and is inserted between conventional interleaved boost converters to form a modified boost fly back forward interleaved structure.

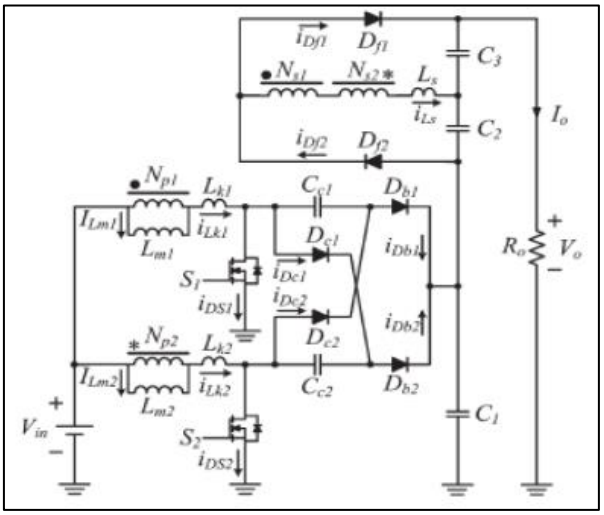

Fig. 4: Circuit diagram of the proposed converter.

B. Operating Principle:

When the switches turn off by turn, the phase whose switch is in OFF state performs as a fly back converter, and the other phase whose switch is in ON state performs as a forward converter. Primary windings of the coupled inductors with N_p turns are employed to decrease input current ripple, and secondary windings of the coupled inductors with N_s turns are connected in series to extend voltage gain. The turn ratios of the coupled inductors are the same. The coupling references of the inductors are denoted by " · " and " * ".

The circuit of the proposed converter is shown in Fig.4.1. Where L_{m1} and L_{m2} are the magnetizing inductors; L_{k1} and L_{k2} represent the leakage inductors; L_s represents the series leakage inductors in the secondary side; S_1 and S_2 denote the power switches; C_{c1} and C_{c2} are the switched capacitors; and C_1, C_2, and C_3 are the output capacitors. D_{c1} and D_{c2} are the clamp diodes, D_{b1} and D_{b2} represent the output diodes for boost operation with switched capacitors, D_{f1} and D_{f2} represent the output diodes for fly back forward operation, and n is defined as turn ratio N_s/N_p. In the circuit analysis, the proposed converter operates in continuous conduction mode (CCM), and the duty cycles of the power switches during steady operation are greater than 0.5 and are interleaved with a 180◦ phase shift. The key steady waveform in one switching period of the proposed converter contains six modes.

1) Mode: 1

I_{kn} mode 1 operation $[t_0, t_1]$, at $t = t_0$, the power switch S_2 remains in ON state, and the other power switch S_1 begins to turn on. The diodes D_{c1}, D_{c2}, D_b1, D_{b2}, and D_{f1} are reversed biased, as shown in Fig. The series leakage inductors Ls quickly release the stored energy to the output terminal via fly back forward diode D_{f2}, and the current through series leakage inductors L_s decreases to zero. Thus, the magnetizing inductor Lm1 still transfers energy to the secondary side of coupled inductors. The current through leakage inductor L_{k1} increases linearly and the other current through leakage inductor L_{k2} decreases linearly.

2) Mode: 2

In this mode $[t_1, t_2]$: At $t = t_1$, both of the power switches S_1 and S_2 remain in ON state, and all diodes are reversed biased. Both currents through leakage inductors L_{k1} and L_{k2} are increased linearly due to charging by input voltage source V_{in}.

3) Mode: 3

In this mode $[t_2, t_3]$ at $t = t_2$, the power switch S1 remains in ON state, and the other power switch S_2 begins to turn off. The diodes D_c1, D_b1, and D_f2 are reversed biased. The energy stored in magnetizing inductor L_{m2} transfers to the secondary side of coupled inductors, and the current through series leakage inductors Ls flows to output capacitor C_3 via fly back forward diode D_{f1}. The voltage stress on power switch S_2 is clamped by clamp capacitor C_{c1} which equals the output voltage of the boost converter. The input voltage source, magnetizing inductor L_{m2}, leakage inductor L_{k2}, and clamp capacitor C_{c2} release energy to the output terminal; thus, V_{c1} obtains a double output voltage of the boost converter.

4) Mode: 4

In this mode $[t_3, t_4]$ at $t = t_3$, the current i_{Dc2} has naturally decreased to zero due to the magnetizing current distribution, and hence, diode reverse recovery losses are alleviated and conduction losses are decreased. Both power

switches and all diodes remain in previous states except the clamp diode D_{c2}.

5) Mode: 5

In this Mode [t_4, t_5] at t = t_4, the power switch S_1 remains in ON state, and the other power switch S2 begins to turn on. The diodes D_{c1}, D_{c2}, D_{b1}, D_{b2}, and Df2 are reversed biased. The series leakage inductors Ls quickly release the stored energy to the output terminal via fly back forward diode D_{f1}, and the current through series leakage inductors decreases to zero. Thus, the magnetizing inductor L_{m2} still transfers energy to the secondary side of coupled inductors. The current through leakage inductor L_{k2} increases linearly and the other current through leakage inductor L_{k1} decreases linearly.

6) Mode: 6

In this Mode [t_5, t_6] at t = t_5, both of the power switches $S_1$and S_2 remain in ON state, and all diodes are reversed biased, as shown in Fig. 5(f). Both currents through leakage inductors L_{k1} and L_{k2} are increased linearly due to charging by input voltage source V_{in}.

7) Mode: 7

In this mode [t_6, t_7] at, t = t_6, the power switch S_2 remains in ON state, and the other power switch S_1 begins to turn off. The diodes D_{c2}, D_{b2}, and D_{f1} are reversed biased. The energy stored in magnetizing inductor Lm1 transfers to the secondary side of coupled inductors, and the current through series leakage inductors flows to output capacitor C_2 via fly back forward diode D_{f2}. The voltage stress on power switch S1 is clamped by clamp capacitor Cc2 which equals the output voltage of the boost converter. The input voltage source, magnetizing inductor L_{m1}, leakage inductor L_{k1}, and clamp capacitor C_{c1} release energy to the output terminal; thus, V_{C1} obtains double output voltage of the boost converter

8) Mode: 8

In this mode [t_6, t_7] at, t = t_6, the power switch S_2 remains in ON state, and the other power switch S1 begins to turn off. The diodes D_{c2}, D_{b2}, and D_{f1} are reversed biased. The energy stored in magnetizing inductor L_{m1} transfers to the secondary side of coupled inductors, and the current through series leakage inductors flows to output capacitor C_2 via fly back forward diode D_{f2}.

The voltage stress on power switch S_1 is clamped by clamp capacitor C_{c2} which equals the output voltage of the boost converter. The input voltage source, magnetizing inductor L_{m1}, leakage inductor L_{k1}, and clamp capacitor C_{c1} release energy to the output terminal; thus, V_{c1} obtains double output voltage of the boost converter.

C. Steady-State Analysis:

The transient characteristics of circuitry are disregarded to simplify the circuit performance analysis of the proposed converter in CCM, and some formulated assumptions are as follows.

- All of the components in the proposed converter are ideal.
- Leakage inductors L_{k1}, L_{k2}, and L_s are neglected.
- Voltages on all capacitors are considered to be constant because of infinitely large capacitance.
- Due to the completely symmetrical interleaved structure, the related components are defined as the corresponding symbols such as D_{c1} and D_{c2} defined as D_c

1) Step Up Gain:

The voltage on clamp capacitor C_c can be regarded as an output voltage of the boost converter. Thus, voltage V_{Cc} can be derived from,

$$V_{Cc} = \frac{1}{1-D} V_{in} \qquad (4.1)$$

When one of the switches turns off, voltage V_{C1} can obtain a double output voltage of the boost converter derived from,

$$V_{c1} = \frac{1}{1-D} V_{in} + V_{Cc} = \frac{2}{1-D} V_{in} \qquad (4.2)$$

The output filter capacitors C_2 and C_3 are charged by energy transformation from the primary side. When S_2 is in ON state and S_1 is in OFF state, V_{C2} is equal to the induced voltage of N_{s1} plus the induced voltage of N_{s2}, and when S_1 is in ON state and S_2 is in OFF state, V_{C3} is also equal to the induced voltage of N_{s1} plus the induced voltage of N_{s2}. Thus, voltages V_{C2} and V_{C3} can be derived from,

$$V_{c2} = V_{c3} = n.\ V_{in}\left(1+\frac{D}{1-D}\right) = \frac{n}{1-D} V_{in} \qquad (4.3)$$

The output voltage can be derived from,

$$V_o = V_{c1}+V_{c2}+V_{c3} = \frac{2n+2}{1-D} V_{in} \qquad (4.4)$$

In addition, the voltage gain of the proposed converter is,

$$\frac{Vo}{Vin} = \frac{2n+2}{1-D} \qquad (4.5)$$

Equation (4.5) confirms that the proposed converter has a high step-up voltage gain without an extreme duty cycle. When the duty cycle is merely 0.6, the voltage gain reaches ten at a turn ratio n of one; the voltage gain reaches 30 at a turn ratio n of five.

D. Voltage Stress on Semiconductor Component:

The voltage ripples on the capacitors are ignored to simplify the voltage stress analysis of the components of the proposed converter. The voltage stress on power switch S is clamped and derived from,

$$Vs1 = Vs2 = \frac{2}{1-D} Vin = \frac{1}{2n+2} Vo \qquad (4.6)$$

Equation (4.6) confirms that low-voltage-rated MOSFET with low RDS (ON) can be adopted for the proposed converter to reduce conduction losses and costs. The voltage stress on the power switch S accounts for a fourth of output voltage V_o, even if turn ratio n is one. This feature makes the proposed converter suitable for high step-up and high-power application.

The voltage stress on diode Dc is equal to V_{C1}, and the voltage stress on diode D_b is voltage V_{C1} minus voltage V_{Cc}. These voltage stresses can be derived from,

$$V_{Dc1} = V_{Dc2} = \frac{2}{1-D} V_{in} = \frac{1}{n+1} V_o \qquad (4.7)$$

$$V_{Db1} = V_{Db2} = V_{c1}-V_{c2} = \frac{1}{1-D} V_{in} = \frac{1}{2n+2} V_o \qquad (4.8)$$

The voltage stress on diode D_b is close to the voltage stress on power switch S. Although the voltage stress on diode D_c is larger, it accounts for only half of output voltage V_o at a turn ratio n of one. The voltage stresses on the diodes are lower as the voltage gain is extended by increasing turn ratio n. The voltage stress on diode D_f equals the V_{C2} plus V_{C3}, which can be derived from,

$$V_{Df1} = V_{Df2} = \frac{2n}{1-D} V_{in} = \frac{n}{n+1} V_o \qquad (4.9)$$

Although the voltage stress on the diode D_f increases as the turn ratio n increases, the voltage stress on

the diodes D_f is always lower than the output voltage. The relationship between the voltage stresses on all the semiconductor components and the turn ratio n.

E. Analysis of Conduction Losses:

Some conduction losses are caused by resistances of semiconductor components and coupled inductors. Thus, all the components in the proposed converter are not assumed to be ideal, except for all the capacitors. Diode reverse recovery problems, core losses, switching losses, and the equivalent series resistance of capacitors are not discussed in this section. The characteristics of leakage inductors are disregarded because of energy recycling.

The equivalent circuit, which includes the conduction losses of coupled inductors and semiconductor components, is shown in Fig. 4.10, in which r_{L1} and r_{L2} are the copper resistances of the primary windings of the coupled inductor, I_{Ls} represents the copper resistances of the secondary windings of the coupled inductors, r_{DS1} and r_{DS2} denote the on-resistances of power switches; V_{Dc1}, V_{Dc2}, V_{Db1}, V_{Db2}, V_{Df1}, and V_{Df2} denote the forward biases of the diodes; and r_{Dc1}, r_{Dc2}, r_{Db1}, r_{Db2}, r_{Df1}, and r_{Ss} are the resistances of the diodes.

Small-ripple approximation was used to calculate conduction losses. Thus, all currents that pass through components were approximated by the dc components. The magnetizing currents and capacitor voltages are assumed to be constant because of the infinite values of magnetizing inductors and capacitors. Finally, through voltage-second balance and capacitor-charge balance, the voltage conversion ratio with conduction losses can be derived from

$$\frac{Vo}{Vin} = \frac{\frac{2n+2}{1-D} - \frac{1}{Vin}.(VDc+VDb+2VDf)}{1+\frac{(2d-1).r_W+r_Z}{Ro(1-D)^2} + \frac{[(2D-1).r_W]+r_Z}{Ro(1-D)}} \quad (4.10)$$

Where,

$$r_w = [2(2-D)(n+1)-1.5]\, r_{Ds} + 4n(1-D)r_{DC} \quad (4.11)$$

$$r_w = 2n(2n+1)\, r_{Ds} + (2n+2)(2^{nD}+2D-1)r_L \quad (4.12)$$

$$r_s = 2(1-2n)\, r_{Dc} + 0.5 r_{Db} \quad (4.13)$$

$$r_w = 4n^2 r_L + 2(r_{Ls} + r_{Df}) \quad (4.14)$$

Because the turn ratio n and copper resistances of the secondary windings of the coupled inductors are directly proportional, the copper resistances of the coupled inductors can be expressed as,

$$r_{Ls} = 2n.\, r_L \quad (4.15)$$

Efficiency is expressed as follows:

$$\eta = \frac{1-\frac{1-D}{(2n+2)}\frac{1}{Vin}.(VDc+VDb+2VDf)}{1+\frac{(2d-1).r_W+r_Z}{Ro(1-D)^2} + \frac{[(2D-1).r_W]+r_Z}{Ro(1-D)}} \quad (4.16)$$

On the basis of (4.11), it can be inferred that the efficiency will be higher if the input voltage is considerably higher than the summation of the forward biases of all the diodes or if the resistance of the load is substantially larger than the resistances of coupled inductors and semiconductor components. In addition, the maximal effect for efficiency is duty cycle, and the secondary is the copper resistance of coupled inductors.

F. Performance of Current Distribution:

The inherent configuration of the proposed converter makes the energy stored in magnetizing inductors transfer via three respective paths as one of the switches turns off. Thus, the current distribution decreases the conduction losses by lower effective value of current and increases the capacity by lower peak value of current. In addition, if the load is not heavy enough, currents through some diodes decrease to zero before they turn off, which alleviate diode reverse recovery losses.

Under light-/medium-load condition, the currents through diodes D_b and D_c decrease to zero before they turn off. When the load is continuously added, only the current I_{Dc} decreases to zero before diode Dc turns off. Under heavy load, although every current through the diode cannot decrease to zero before the related diode turns off, the reduction of conduction losses and the increase of capacity still perform well.

IV. SIMULATION OF PROPOSED SYSTEM

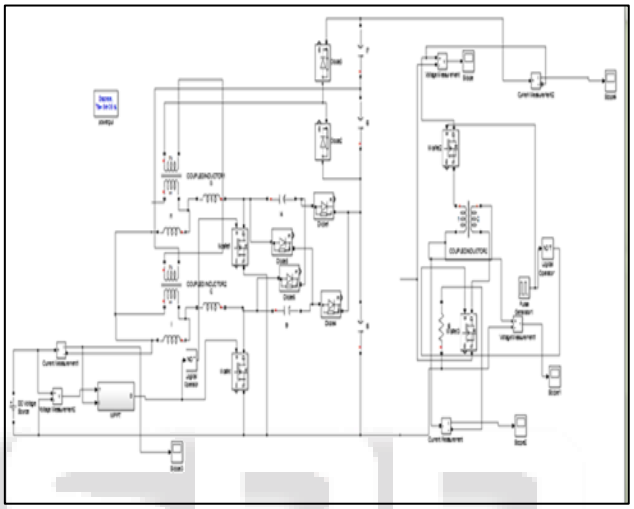

Fig. 5: Simulation of Proposed system

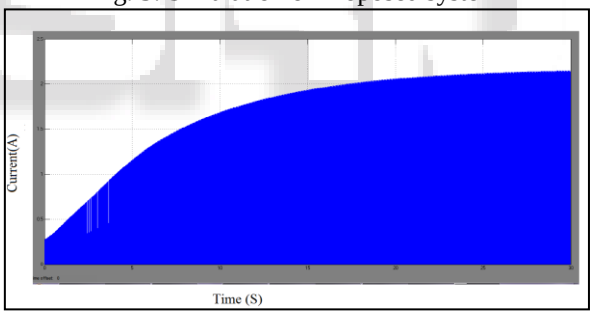

Fig. 6: Output DC Current

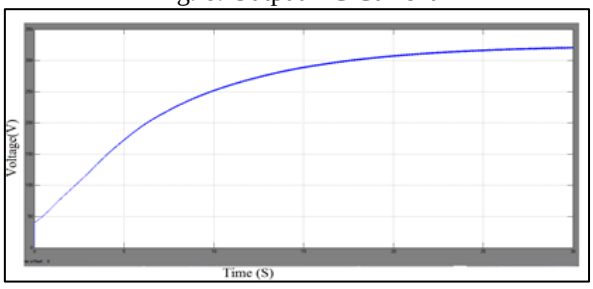

Fig. 7: Output DC voltage

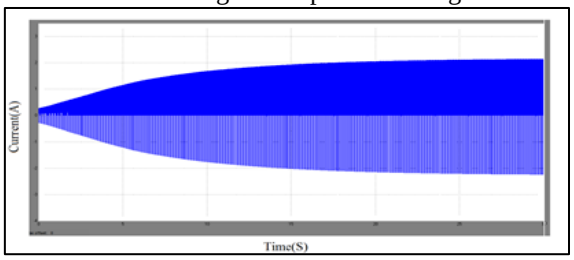

Fig. 8: AC Out Put Current

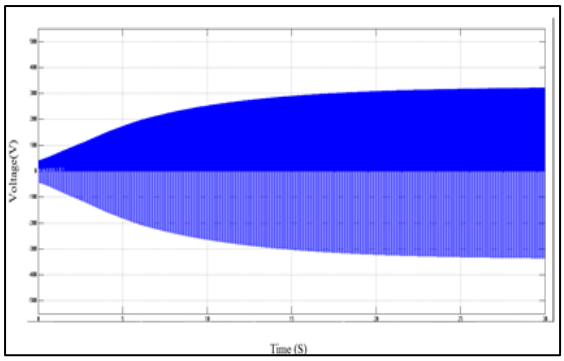

Fig. 9: AC Out Put Voltage

V. CONCLUSION

This paper has presented the theoretical analysis of steady state, related consideration, and simulation results for the proposed converter using the Incremental Conductance MPPT. Proposed converter has successfully implemented an efficient high step-up conversion through the voltage multiplier module. The interleaved structure reduces the input current ripple and distributes the current through each component. In addition, the lossless passive clamp function recycles the leakage energy and constrains a large voltage spike across the power switch. A grid connected application is possible through the efficient inverter connection. Meanwhile, the voltage stress on the power switch is restricted and much lower than the output voltage (380 V). Furthermore, the full-load efficiency is 96.4% at P_o = 1000 W, and the highest efficiency is 97.1% at Po = 400 W. Thus, the proposed converter is suitable for high-power or renewable energy applications that need high step-up conversion.

VI. ACKNOWLEDGEMENT

First and Foremost, I owe my colossal gratitude to the ALMIGHTY SGOD for blessing me with his grace and taking my endeavor to a successful culmination. I am highly obliged to express my sense of gratitude to the Principal of our institution Dr. George Chellian Chandran, B.E., M.E., Ph.D., PGDBM, Head of the Department Prof.P. Pradeepa, B.E., M.E., (Ph.D)., andto my guide Miss.S. Monica, B.E.,M.E.,Asst. Professor, Electrical and Electronics Engineering.

REFERENCES

[1] Kuo-Ching Tseng and Chi-Chih, "Huang High Step-Up High-Efficiency Interleaved Converter with Voltage Multiplier Module for Renewable Energy System", IEEE Transactions on Industrial Electronics, vol. 61, no. 3, march 2014.
[2] C. M. Lai, C. T. Pan, and M. C. Cheng, "High-efficiency modular high step-up interleaved boost converter for DC micro grid applications," IEEE Trans. Ind. Appl., vol. 48, no. 1, pp. 161–171, Jan./Feb. 2012.
[3] W. Li, Y. Zhao, J. Wu, and X. He, "Interleaved high step-up converter with winding-cross-coupled inductors and voltage multiplier cells," IEEE Trans. Power Electron., vol. 27, no. 1, pp. 133–143, Jan. 2012.
[4] J. T. Bialasiewicz, "Renewable energy systems with photovoltaic power generators: Operation and modeling," IEEE Trans. Ind. Electron., vol. 55, no. 7, pp. 2752–2758, Jul. 2008.
[5] T. Kefalas and A. Kladas, "Analysis of transformers working under heavily saturated conditions in grid connected renewable energy systems," IEEE Trans. Ind. Electron., vol. 59, no. 5, pp. 2342–2350, May 2012.
[6] T. Zhou and B. Francois, "Energy management and power control of a hybrid active wind generator for distributed power generation and grid integration," IEEE Trans. Ind. Electron., vol. 58, no. 1, pp. 95–104, Jan. 2011.
[7] M. Veerachary, T. Senjyu, and K. Uezato, "Neural-network-based maximum-power-point tracking of coupled-inductor interleaved-boostconverter boost converter supplied PV system using fuzzy controller," IEEE Trans. Ind.Electron., vol. 50, no. 4, pp. 749–758, Aug. 2003.
[8] B. Liu, S. Duan, F. Liu, and P. Xu, "Analysis and improvement of maximum power point tracking algorithm based on incremental conductance method for photovoltaic array," in Proc. IEEE PEDS, 2007, pp. 637–641.

